Lab on a Chip

COMMUNICATION

A similarity scaling approach for organ-on-chip devices†

James J. Feng *[ab] and Sarah Hedtrich [cde]

Cite this: *Lab Chip*, 2022, **22**, 3663

Received 12th July 2022,
Accepted 30th August 2022

DOI: 10.1039/d2lc00641c

rsc.li/loc

Organ-on-chip devices (OoCs) provide more nuanced insights into (patho)physiological processes of the human body than static tissue models, and are currently the most promising approach to emulating human (patho)physiology *in vitro*. OoC designs vary greatly and questions remain as to how to maximize biomimicry and clinical translatability of the *in vitro* findings. Scaling is critical, yet has largely been *ad hoc*, consisting in matching one or a few variables between the OoC and the target organ. This has limited the predictive value of OoCs. Here, we propose a systematic approach based on the principle of similitude widely used in the physical sciences, and present three case studies from the recent literature to demonstrate how the approach works. A lung-on-a-chip and a liver-on-a-chip both satisfied important similarity criteria, and therefore yielded results that were in good agreement with clinical data. A gut–liver system failed to satisfy a key criterion of kinematic similarity, and yielded unphysiological pharmacokinetic responses *in vitro*. The similarity scaling approach promises to improve markedly the design and operation of organ- and human-on-chip devices.

Introduction

The past decade has seen intensifying efforts to develop complex *in vitro* models that closely replicate functions of human organs.[1,2] These typically involve multiple cell types assembled in three dimensions to mimic the morphology and functionality of the target organs, and are popularly known as "organ-on-chip" (OoC) devices or microphysiological systems (MPS).[3–5] Such OoCs can be assembled into a multi-organ-on-chip system to study inter-organ crosstalk.[6–8] OoCs emulate organ-level (patho)physiology and are currently the most promising human-based approach in biomedical research. Much of this research has been motivated by the prospect of using OoCs to improve clinical translation and reduce attrition rate in the drug development process, potentially replacing animal testing.[2,3,5,9–13]

For a miniaturized on-chip culture to mimic a human organ, scaling is a central issue: how to design OoCs so that their performance *in vitro* can be extrapolated to the functions of organs *in vivo*? Existing approaches are mostly *ad hoc*, focusing on specific parameters or functions in a specific OoC. In particular, they do not account systematically for the many interlinked mechanisms and parameters in OoCs. For example, direct scaling[14] and allometric scaling[15] use the OoC-to-human size or mass ratio to determine the size of the organs on the chip. Such scalings do not involve any time scales, and cannot ensure proper scaling of rate parameters (*e.g.*, perfusion and metabolic rates). In a gut–liver system, direct or allometric scaling would produce drug exposure times that are orders of magnitude below *in vivo*.[16] Functional scaling strives for *in vivo* levels of key functions for each organ, *e.g.*, metabolic rate for the liver or filtration rate for the kidney.[17,18] But the difficulty lies in balancing the often conflicting needs of multiple functions, especially in multiple OoCs setups.[6,16] From the earlier years of OoC development, scaling has been recognized as an outstanding problem.[3,17,19,20] But a general framework for scaling remains elusive, and recent reviews have consistently listed scaling as an urgent problem to be tackled.[1,8,21,22]

We argue that the solution requires a shift in focus from the *ad hoc* needs of specific OoCs to a systematic view that accounts for the multiple factors involved. Here we propose one such framework by adapting the techniques of dimensional analysis and similarity, both classical tools in physics and engineering.

[a] *Department of Chemical and Biological Engineering, University of British Columbia, Vancouver, BC V6T 1Z4, Canada. E-mail: james.feng@ubc.ca*
[b] *Department of Mathematics, University of British Columbia, Vancouver, BC V6T 1Z2, Canada*
[c] *Department of Infectious Diseases and Respiratory Medicine, Charité – Universitätsmedizin Berlin, Corporate member of Freie Universität Berlin and Humboldt Universität zu Berlin, Germany*
[d] *Center of Biological Design, Berlin Institute of Health at Charité – Universitätsmedizin Berlin, Germany*
[e] *Faculty of Pharmaceutical Sciences, University of British Columbia, Vancouver, BC V6T 1Z3, Canada*

† Electronic supplementary information (ESI) available. See DOI: https://doi.org/10.1039/d2lc00641c

Similarity scaling

In any physical process, if the *output* P is determined by *input* quantities q_i (i = 1,…, n), then these inputs must be algebraically linked in such a way as to yield the proper dimension of P. The pi theorem[23] asserts that the relationship among P and q_i can be reduced, without any loss of generality, to one among a smaller number of independent dimensionless Π groups, each formed by products of powers of P and q_i. This relationship then forms the basis for scaling between a *model* and its *prototype*. The procedure is widely used in scale-up in physics and engineering,[24,25] and the ESI† offers an example in aeronautics.

For an OoC, we first identify the key output P that is to be translated to *in vivo*. Then the Π group Π_1 that represents P must be a function of the other Π groups, Π_2,…, Π_m,

$$\Pi_1 = f(\Pi_2, \Pi_3, \ldots, \Pi_m),$$

with the total number $m < n + 1$. If we ensure that the inputs Π_2,…, Π_m for the OoC match those *in vivo*, the output Π_1 must be matched as well. Thus, we have achieved *similarity* between the OoC and its target organ, and the *in vitro* measurement of P can be translated to the *in vivo* organ. Notably, this does not require knowledge of the function f, which is almost always unknown in a complex system. The procedure can be extended to multiple output functions for a single OoC, or to multi-organ chips.

Similarity criteria

When scaling mechanical systems, one sometimes classifies the dimensionless groups according to geometric, kinematic and dynamic similarity.[26,27] Geometric similarity governs the Π groups describing length, area and volume ratios, angles and shapes. Such ratios must be equal between the model and the prototype. Kinematic similarity requires equality of time-scale ratios in addition to length ratios. Thus, it concerns Π groups that involve velocity and other rate quantities. On the basis of these two, dynamic similarity further introduces mass ratios so that dynamic quantities such as pressure, shear stresses and forces, which typically constitute the output Π groups in a mechanical system, are scaled properly.

This scheme can be adapted and expanded for scaling OoCs. The Π groups about OoC size, shape and volume pertain to geometric similarity, those about residence time, perfusion rates and kinetic rates belong to kinematic similarity, and finally those involving forces and stresses fall under dynamic similarity. For OoCs, we need to add *morphological similarity* as a new criterion, which ensures the proper structure and morphology of heterotypic cell assemblies, *e.g.*, to distinguish spheroids from dispersed cells, and predominantly 2D from 3D structures.[19,28] Finally, metabolic outcomes such as concentration profiles are central to pharmacokinetic/pharmacodynamic (PKPD) studies using OoCs.[16,29,30] Thus, we propose another new criterion called *metabolic similarity* that ensures proper scaling of dosage and concentrations.

It is also interesting to note that some of the *ad hoc* scaling schemes proposed in earlier work[8,16,18,19] may be identified with the similarity criteria above. For example, requirements on chamber size ratio and cell number are for geometric similarity. Requirements on perfusion rates, metabolic rates, organ- or cell-to-liquid ratios and residence time concern kinematic similarity, and requirement on shear stress concerns dynamic similarity. Thus, in carrying out the proposed similarity scaling, one may also satisfy some such *ad hoc* criteria by accident.

Partial similarity

In principle, the pi theorem guarantees similarity. In the laboratory, however, complete similarity may not be attainable because of limitations on the materials available, fabrication techniques and accessible experimental conditions. In such cases, one strategically omits certain Π groups and strives for partial similarity.[23] This is often necessary even for mechanical systems. In the OoC, we may have to determine which input Π's are more or less important for the phenomena of interest, and carry out scaling based on partial similarity. In multi-organ chips, the greater complexity implies a larger number of Π groups. Although the principle of similarity scaling applies to such systems, partial similarity may become unavoidable.

Case studies

Similarity scaling differs from prior scaling methods in that it accounts for all parameters and their interactions in a systematic way. Although OoCs are vastly more complex than mechanical systems, we show here that the success of similarity scaling in the latter can be reproduced in the former, provided that the OoC experiments are designed and executed properly. For this purpose, we have selected three studies from the literature based on the completeness of the reported parameters, operating conditions, and quantitative outputs for their respective OoCs. The availability of such data make them proper test cases for the similarity scaling approach.

Lung-on-a-chip (LOAC)

Huh *et al.*[31,32] developed the LOAC as a mimic for an alveolus. It features an air–liquid interface that can be cyclically stretched to replicate the alveolar stretching during breathing. As a disease model for pulmonary edema due to cancer treatment by interleukin-2, the LOAC manifests a gradual loss of barrier function; the increase in permeability agrees well with *ex vivo* data from whole mouse lungs.[32]

To examine the success of LOAC from the angle of similarity scaling, we take the permeability to be the output that depends on a host of input variables and parameters, including the drug dosage, the frequency and amplitude of

membrane stretching, and the medium perfusion velocity. Our dimensional analysis (see ESI† for details) produces 6 Π groups, with the output $\Pi_1 = k/D^2$ being the ratio of the membrane permeability to the chamber width squared. The authors have matched the Π groups between the LOAC and *in vivo*. In particular, the following similarity criteria are satisfied:

- Geometric similarity: the LOAC matches the chamber size and the air–liquid-interface thickness with the alveolus *in vivo*.
- Morphological similarity: the LOAC has confluent endothelial and epithelial monolayers apposed on either side of the membrane, approximating the air-blood boundary *in vivo*.
- Kinematic similarity: the membrane stretching amplitude, frequency and the medium perfusion velocity are all chosen to match the *in vivo* conditions.
- Metabolic similarity: the interleukin-2 dosage and application time are matched with *in vivo* conditions.

Thus, the LOAC and the operating conditions of Huh *et al.*[32] have achieved similarity with the *in vivo* counterpart. This ensures that the output of the LOAC, the membrane permeability enhanced by interleukin-2 treatment, is translatable from the LOAC to the alveolus. Note that this is a somewhat special case of 1 : 1 size ratio between the model and the prototype. Moreover, all the Π groups are matched for a rare attainment of complete similarity.

More recently, second-generation LOACs have been developed that continue to maintain similarity scaling with a 1 : 1 size ratio, but with improved and refined features, including the use of primary alveolar epithelial cells instead of a cell line[33] and the modeling of cytokine production and leukocyte recruitment following an influenza infection.[34]

Liver-on-a-chip

Ewart *et al.*[35] studied drug-induced liver injury (DILI) on a Liver-Chip, an OoC that models a liver sinusoid. Judging by suppressed albumin production and other symptoms, the OoC distinguished toxic drugs from their non-toxic structural analogs, and correctly ordered the toxicity of drugs according to the Garside DILI rank. We will demonstrate below that this success is again rooted in satisfying similarity scaling to the *in vivo* organ, which is the human liver sinusoid in this case.

The details of the dimensional analysis can be found in the ESI,† and only a brief summary is given below. Without drug treatment, the Liver-Chip produces albumin *in vitro* in the physiologic *in vivo* range of 20–105 μg per 10^6 hepatocytes per day. In the DILI study, therefore, the main output is the albumin production as a fraction of the control without drug treatment: $\Pi_1 = \phi$. The input variables and parameters are listed in Table 1, along with the values of the input Π groups, $\Pi_2,\ldots, \Pi_5$. Of these, Π_2, Π_3 and Π_4 match reasonably well between *in vitro* and *in vivo*. Π_5 differs considerably, but its small magnitudes suggest that permeation through the cell layers happens rapidly, and is not the rate-limiting step. Thus, we can disregard Π_5 and claim partial similarity between the Liver-Chip and the liver sinusoid *in vivo*. This ensures translatability of albumin suppression $\Pi_1 = \phi$, and therefore the proper detection of DILI.

Table 1 Similarity scaling for the Liver-Chip in a DILI study.[35] The input parameters are *L*: chip dimension, *u*: perfusion velocity, *c*: initial drug concentration, c_{50}: required drug concentration to produce a 50% reduction in albumin, *D*: drug diffusivity in perfusate, *P*: permeability through the membrane, *k*: drug clearance rate. The various rates are for the drug diclofenac. See ESI† for details of dimensional analysis and the sources for the parameter values

Parameters	*In vitro* values	*In vivo* values
L (μm)	200	5
u (μm min^{-1})	2500	6.67×10^4
k (μm^3 min^{-1})	1.67×10^9	2.93×10^7
D (μm^2 min^{-1})	4.50×10^4	4.50×10^4
P (μm min^{-1})	6.53×10^6	6.53×10^6
c (μM)	0.05	0.05
c_{50} (μM)	0.1	0.1
$\Pi_2 = c/c_{50}$	0.5	0.5
$\Pi_3 = \mathrm{uL}^2/k$	5.99×10^{-2}	5.69×10^{-2}
$\Pi_4 = \mathrm{uL}/D$	11.1	7.41
$\Pi_5 = \mathrm{u}/P$	3.83×10^{-4}	1.02×10^{-2}

Even though the Liver-Chip is much larger than the liver sinusoid *in vivo*, the perfusion and drug clearance rates also differ so as to compensate through the Π groups. This systematic treatment is the principal advantage of similarity scaling over prior scaling that focuses on matching individual parameters.

Gut–liver system

Cirit *et al.*[16,36,37] linked a gut and a liver module into a multi-OoC system that captured the key functions of both organs—the permeation of orally administered drugs across the membrane in the gut and drug metabolism in the liver—as well as their crosstalk. The gut OoC has an apical chamber and a basolateral chamber, but the liver OoC has a single chamber. Both are connected to a mixing chamber that supplies the common perfusion. This system has been used to study drug metabolism in a multi-organ system.[16,37]

The system involves a larger number of parameters, and requires a lengthier dimensional analysis resulting in 12 Π groups (details in ESI†). For the present purpose, we need only discuss the parameters and Π groups relevant to kinematic similarity, more specifically the transport and kinetic rates. These are listed in Table 2 for the drug diclofenac. The dimensionless groups Π_6 and Π_7 indicate the gut and liver metabolic rates of the drug relative to its transport rate by perfusion. Π_8 gives the ratio between the drug permeation and perfusion. The small values of C_g and Π_6 indicate negligible drug metabolism in the gut. The most prominent discrepancy is in $\Pi_7 = C_l/Q$, which is more than 10 000 times greater *in vitro* than *in vivo*. This severely violates the kinematic similarity.[23] Π_7 is also the ratio between the circulation time $T_0 = V_m/Q$ and the liver clearance time $T_l = V_m/C_l$. Not only is the circulation too slow

Table 2 Similarity scaling for a gut–liver OoC system,[16,37] with a partial list of the rate parameters: C_l and C_g: diclofenac clearance rates in liver and gut, P: membrane permeability, Q: perfusion rate, S: membrane area, V_m: volume of mixing chamber, T_0: circulation time, T_l: liver clearance time. See ESI† for details of dimensional analysis and the sources for the parameter values

Parameters	*In vitro* values	*In vivo* values
C_l (mL min^{-1})	0.0102	0.0813
C_g (mL min^{-1})	0.00029	0
P (cm min^{-1})	8.83×10^{-4}	1.08×10^{-3}
Q (mL min^{-1})	0.0104	1250
S (cm^2)	1.12	3×10^5
V_m (mL)	1	1750
$\Pi_6 = C_g/Q$	0.0279	0
$\Pi_7 = C_l/Q$	0.980	6.50×10^{-5}
$\Pi_8 = PS/Q$	0.0951	0.259
$T_0 = V_m/Q$ (min)	96.1	1.40
$T_l = V_m/C_l$ (min)	98.0	21 525

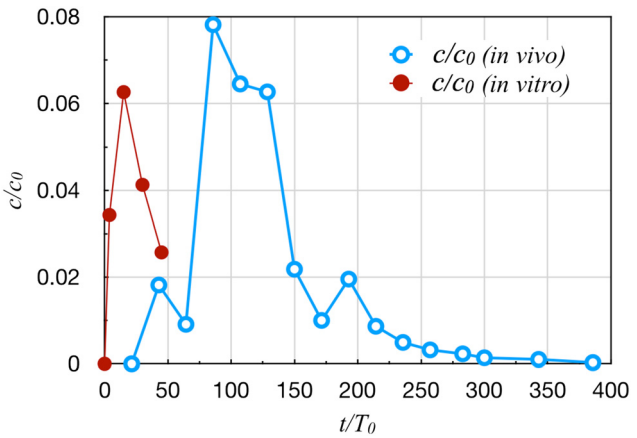

Fig. 1 Comparison of the plasma diclofenac concentration profiles *in vivo*[16] and *in vitro*.[37] Time t is scaled by the circulation time T_0, and concentration c by the initial concentration c_0 in the dosing chamber.

in vitro, the clearance is also too fast. As a result, the time concentration profile fails to translate to the clinical data, with a much shorter time scale than *in vivo* (Fig. 1).[16]

Similarity scaling not only pinpoints the cause of the mis-scaling, but can also suggest ways to correct it. Since C_l depends on the metabolism of individual cells, it cannot be easily varied *in vitro*. Thus one can only raise the perfusion rate Q to lower Π_7. To maintain the value of Π_8, already roughly matched with *in vivo*, one must increase the gut epithelial area S in proportion to Q. This systematic approach to managing the parameters is the hallmark of similarity scaling.

Discussion

Similarity scaling offers a systematic scheme for matching OoCs and their target organs, as opposed to matching individual parameters. It is also mathematically guaranteed to work by the pi theorem. In practice, limitations in available materials and fabrication techniques often make complete similarity impossible. But even partial similarity can provide highly useful guidelines, as demonstrated in the above.

OoCs being biological systems puts special constraints on similarity scaling. An individual cell is in a sense the minimum unit and cannot be scaled further down. Thus, an OoC typically contains a smaller number of the same cells as *in vivo*, not the same number of "smaller cells" as perfect similarity would dictate. Moreover, certain parameters, *e.g.*, cellular metabolic rates, will be more or less fixed at their *in vivo* values and not subject to large variations for scaling. Despite these limitations, we have shown the utility and potential of similarity scaling in the case studies. It will offer a general framework for designing the next generation of organ- and human-on-chip systems.

Materials and methods

The method of dimensional analysis is illustrated with examples in the ESI,† which also contains detailed analysis and all the data for the three case studies.

Author contributions

JJF and SH conceptualized the project, carried out the investigation, analyzed the data and wrote the paper.

Conflicts of interest

There are no conflicts to declare.

Acknowledgements

We acknowledge partial funding of this work from the Stiftung Charité (S. H.), the Natural Sciences and Engineering Research Council Canada (2020-04224 for S. H., 2019-04162 for J. J. F.), the German Research Foundation (DFG, SFB 1449-431232613, project A5, S. H.), and the John R. Evans Leaders Fund (S. H.). J. J. F. thanks Milica Radisic (University of Toronto) for suggesting the scaling problem to him. The image in the online "Table of Contents" entry was partly generated using Servier Medical Art, provided by Servier, licensed under a Creative Commons Attribution 3.0 unported license.

Notes and references

1 G. Vunjak-Novakovic, K. Ronaldson-Bouchard and M. Radisic, *Cell*, 2021, **184**, 4597–4611.
2 L. A. Low, C. Mummery, B. R. Berridge, C. P. Austin and D. A. Tagle, *Nat. Rev. Drug Discovery*, 2021, **20**, 345–361.
3 K. Ronaldson-Bouchard and G. Vunjak-Novakovic, *Cell Stem Cell*, 2018, **22**, 310–324.
4 S. E. Park, A. Georgescu and D. Huh, *Science*, 2019, **364**, 960–965.
5 M. Weinhart, A. Hocke, S. Hippenstiel, J. Kurreck and S. Hedtrich, *Pharmacol. Res.*, 2019, **139**, 446–451.
6 J. H. Sung, Y. I. Wang, S. N. Narasimhan, M. Jackson, C. Long, J. J. Hickman and M. L. Shuler, *Anal. Chem.*, 2019, **91**, 330–351.

7 D. Park, J. Lee, J. J. Chung, Y. Jung and S. H. Kim, *Trends Biotechnol.*, 2020, **38**, 99–112.
8 M. Malik, Y. Yang, P. Fathi, G. J. Mahler and M. B. Esch, *Front. Cell Dev. Biol.*, 2021, **9**, 721338.
9 N. T. Elliott and F. Yuan, *J. Pharm. Sci.*, 2011, **100**, 59–74.
10 U. Marx, T. Akabane, T. B. Andersson, E. Baker, M. Beilmann, S. Beken, S. Brendler-Schwaab, M. Cirit, R. David, E. M. Dehne, I. Durieux, L. Ewart, S. C. Fitzpatrick, O. Frey, F. Fuchs, L. G. Griffith, G. A. Hamilton, T. Hartung, J. Hoeng, H. Hogberg, D. J. Hughes, D. E. Ingber, A. Iskandar, T. Kanamori, H. Kojima, J. Kuehnl, M. Leist, B. Li, P. Loskill, D. L. Mendrick, T. Neumann, G. Pallocca, I. Rusyn, L. Smirnova, T. Steger-Hartmann, D. A. Tagle, A. Tonevitsky, S. Tsyb, M. Trapecar, B. Van de Water, J. Van den Eijnden-van Raaij, P. Vulto, K. Watanabe, A. Wolf, X. Zhou and A. Roth, *ALTEX*, 2020, **37**, 365–394.
11 P. P. Adhikary, Q. U. Ain, A. C. Hocke and S. Hedtrich, *Nat. Rev. Mater.*, 2021, **6**, 374–376.
12 B. Cecen, C. Karavasili, M. Nazir, A. Bhusal, E. Dogan, F. Shahriyari, S. Tamburaci, M. Buyukoz, L. D. Kozaci and A. K. Miri, *Pharmaceutics*, 2021, **13**, 1657.
13 K. Ronaldson-Bouchard, D. Teles, K. Yeager, D. N. Tavakol, Y. Zhao, A. Chramiec, S. Tagore, M. Summers, S. Stylianos, M. Tamargo, B. M. Lee, S. P. Halligan, E. H. Abaci, Z. Guo, J. Jacków, A. Pappalardo, J. Shih, R. K. Soni, S. Sonar, C. German, A. M. Christiano, A. Califano, K. K. Hirschi, C. S. Chen, A. Przekwas and G. Vunjak-Novakovic, *Nat. Biomed. Eng.*, 2022, **6**, 351–371.
14 I. Maschmeyer, A. K. Lorenz, K. Schimek, T. Hasenberg, A. P. Ramme, J. Hübner, M. Lindner, C. Drewell, S. Bauer, A. Thomas, N. S. Sambo, F. Sonntag, R. Lauster and U. Marx, *Lab Chip*, 2015, **15**, 2688–2699.
15 A. Ahluwalia, *Sci. Rep.*, 2017, **7**, 42113.
16 C. Maass, C. L. Stokes, L. G. Griffith and M. Cirit, *Integr. Biol.*, 2017, **9**, 290–302.
17 J. P. Wikswo, E. L. Curtis, Z. E. Eagleton, B. C. Evans, A. Kole, L. H. Hofmeister and W. J. Matloff, *Lab Chip*, 2013, **13**, 3496–3511.
18 J. H. Sung, Y. Wang and M. L. Shuler, *APL Bioeng.*, 2019, **3**, 021501.
19 C. Moraes, J. M. Labuz, B. M. Leung, M. Inoue, T.-H. Chun and S. Takayama, *Integr. Biol.*, 2013, **5**, 1149–1161.
20 C. L. Stokes, M. Cirit and D. A. Lauffenburger, *CPT: Pharmacometrics Syst. Pharmacol.*, 2015, **4**, 559–562.
21 P. Sphabmixay, M. S. B. Raredon, A. J.-S. Wang, H. Lee, P. T. Hammond, N. X. Fang and L. G. Griffith, *Biofabrication*, 2021, **13**, 045024.
22 D. E. Ingber, *Nat. Rev. Genet.*, 2022, **23**, 467–491.
23 M. Zlokarnik, *Scale-Up in Chemical Engineering*, WILEY-VCH Verlag, 2nd edn, 2006.
24 A. Bisio and R. L. Kabel, *Scale-up of Chemical Processes: Conversion from Laboratory Scale Tests to Successful Commercial Size Design*, Wiley-Interscience, 1985.
25 J. M. Bonem, *Chemical Projects Scale Up: How to Go from Laboratory to Commercial*, Elsevier, 2018.
26 J. R. Welty, C. E. Wicks, R. E. Wilson and G. L. Rorrer, *Fundamentals of Momentum, Heat, and Mass Transfer*, Wiley, 5th edn, 2008, pp. 125–136.
27 F. M. White, *Fluid Mechanics*, McGraw-Hill, Seventh edn, 2011, pp. 293–345.
28 N. Ucciferri, T. Sbrana and A. Ahluwalia, *Front. Bioeng. Biotechnol.*, 2014, **2**, 74.
29 C. Ma, Y. Peng, H. Li and W. Chen, *Trends Pharmacol. Sci.*, 2021, **42**, 119–133.
30 Y. Yang, Y. Chen, L. Wang, S. Xu, G. Fang, X. Guo, Z. Chen and Z. Gu, *Front. Bioeng. Biotechnol.*, 2022, **10**, 900481.
31 D. Huh, B. D. Matthews, A. Mammoto, M. Montoya-Zavala, H. Y. Hsin and D. E. Ingber, *Science*, 2010, **328**, 1662–1668.
32 D. Huh, D. C. Leslie, B. D. Matthews, J. P. Fraser, S. Jurek, G. A. Hamilton, K. S. Thorneloe, M. A. McAlexander and D. E. Ingber, *Sci. Transl. Med.*, 2012, **4**, 159ra147.
33 P. Zamprogno, S. Wüthrich, S. Achenbach, G. Thoma, J. D. Stucki, N. Hobi, N. Schneider-Daum, C.-M. Lehr, H. Huwer, T. Geiser, R. A. Schmid and O. T. Guenat, *Commun. Biol.*, 2021, **4**, 168–423.
34 H. Bai, L. Si, A. Jiang, C. Belgur, R. Plebani, C. Oh, M. Rodas, A. Nurani, S. Gilpin, R. K. Powers, G. Goyal, R. P. Baun and D. E. Ingber, *Nat. Commun.*, 2022, **13**, 1928.
35 L. Ewart, A. Apostolou, S. A. Briggs, C. V. Carman, J. T. Chaff, A. R. Heng, S. Jadalannagari, J. Janardhanan, K.-J. Jang, S. R. Joshipura, M. Kadam, M. Kanellias, V. J. Kujala, G. Kulkarni, C. Y. Le, C. Lucchesi, D. V. Manatakis, K. K. Maniar, M. E. Quinn, J. S. Ravan, A. C. Rizos, J. F. Sauld, J. Sliz, W. Tien-Street, D. Ramos Trinidad, J. Velez, M. Wendell, P. K. Mahalingaiah, D. E. Ingber and D. Levner, bioRxiv, 2021, preprint, DOI: **10.1101/2021.12.14.472674**.
36 N. Tsamandouras, T. Kostrzewski, C. L. Stokes, L. G. Griffith, D. J. Hughes and M. Cirit, *J. Pharmacol. Exp. Ther.*, 2017, **360**, 95–105.
37 N. Tsamandouras, W. L. K. Chen, C. D. Edington, C. L. Stokes, L. G. Griffith and M. Cirit, *AAPS J.*, 2017, **19**, 1499–1512.

Electronic Supplementary Material (ESI) for Lab on a Chip.

Electronic Supplementary Information (ESI) for

A similarity scaling approach for organ-on-chip devices

James J. Feng[1,2*] and Sarah Hedtrich[3,4,5]

[1] Department of Chemical and Biological Engineering, University of British Columbia, Vancouver, Canada

[2] Department of Mathematics, University of British Columbia, Vancouver, Canada

[3] Department of Infectious Diseases and Respiratory Medicine, Charité - Universitätsmedizin Berlin, corporate member of Freie Universität Berlin and Humboldt Universität zu Berlin, Germany

[4] Center of Biological Design, Berlin Institute of Health at Charité - Universitätsmedizin Berlin, Germany

[5] Faculty of Pharmaceutical Sciences, University of British Columbia, Vancouver, BC, Canada.

The main paper proposes similarity scaling as a systematic method for scaling organ-on-chip (OoC) devices. In the following, we first illustrate the technique of dimensional analysis with an example, and then carry out the detailed analysis for each of the 3 case studies of the main text, with all supporting data.

Dimensional analysis

Dimensional analysis and similarity are widely used in science and engineering [1]. The procedure is underpinned by the pi theorem, and reduces the functional dependence of an output quantity P on the inputs q_1, …, q_n of a problem

$$P = f(q_1, q_2, \ldots, q_n)$$

to an equivalent functional relationship among a smaller number of dimensionless groups, called the Π groups:

$$\Pi_1 = F(\Pi_2, \ldots, \Pi_m),$$

where Π_1 is the dimensionless group containing the output P, and the other Π groups contain the input variables and parameters. The functional form F

* Corresponding author, email: james.feng@ubc.ca

generally differs from *f*, and the second equation involves a smaller number of variables: $m < n + 1$.

Consider a physical or biological systems such as an organ (to be called a "prototype" below), alongside a "model" that is typically a scaled down *in vitro* version of the prototype. The dimensional analysis can be performed on both, resulting in relationships among the Π groups. Provided that the model operates from the same underlying mechanisms and principles as the prototype, the functional form *F* is the same between them. Therefore, if we control the operating conditions and parameters in the model system so that its input Π groups (Π_2, … Π_m) match those of the prototype, then the output Π_1 must match as well:

$$\Pi_1^{model} = \Pi_1^{prototype},$$

which allows us to scale the measured values in the model system to that in the prototype. The model and prototype are said to be in similarity.

The procedure of constructing the Π groups is detailed in textbooks; Zlokarnik [1] is a highly readable one with many examples. The key is to recognize that the dimensions of all the variables and parameters of a problem consist of a few fundamental dimensions such as length, mass, time, temperature, amount of substance and electric charge. Thus, a judicious combination of these variables and parameters, through multiplication, division and exponentiation, will yield a dimensionless group. The total number of dimensionless groups is typically the number of variables and parameters minus the number of fundamental dimensions. All such Π groups can be derived through a systematic and foolproof procedure [1]. In the following, we will illustrate this through an example.

An example from engineering

As an illustration of the procedure, let us consider a classical example from aeronautics. If we design an experiment to study the drag force *D* on an aircraft, we build a model of the plane—much smaller than the prototype—and blow wind over the model in a wind tunnel. Thus, one can measure *D* on the model.

The starting point of the dimensional analysis is to list all the variables and parameters of the problem that may have affected the quantity of main interest that we have measured. Here, we take *D* to be dependent on the air density ρ, air viscosity μ, wind speed *U* and the dimension *d* of the airplane. Of course, there may be multiple dimensions for the airplane, e.g., length, width and height. We use a single dimension *d* for simplicity in this illustration. Thus, we list *D* as the output and the other 4 quantities as inputs: ρ, μ, *U*, *d.*

Next, we express the dimension of each of the variables in terms of the 3 fundamental dimensions of the problem: length (L), time (T) and mass (M). For example, *D* is a force, whose dimension is mass times length divided by time

squared (from Newton's second law of motion): $\{D_f\} = MLT^{-2}$. Similarly we write out the dimensions for all the other variables and parameters, based on the physical meaning of each quantity (e.g., viscosity as defined from the shear stress on a Newtonian fluid):

Outputs: $\{D_f\} = MLT^{-2}$; Inputs: $\{\rho\}=ML^{-3}$, $\{\mu\}=ML^{-1}T^{-1}$, $\{U\}=LT^{-1}$, $\{d\}=L$.

Because there are 3 fundamental dimensions, if we combine 4 quantities together via multiplication, division and exponentiation, we should be able to cancel out the 3 fundamental dimensions to produce a Π group. Let us try this among the 4 inputs:

$$\Pi_2 = \rho^a \mu^b U^c d,$$

with the exponents a, b and c being numbers to be determined. We call this group Π_2 as we have on p. 1 reserved Π_1 for the dimensionless group involving the output quantity (D in this case; see below). Requiring the dimension of Π_2 to vanish gives 3 algebraic equations for a, b and c:

$$\{\Pi_2\}= (ML^{-3})^a (ML^{-1}T^{-1})^b \{LT^{-1}\}^c L = M^0L^0T^0$$

The unique solution is $a = 1$, $b = -1$ and $c = 1$. Thus, we obtain

$$\Pi_2 = \rho U d/\mu,$$

which is known as the Reynolds number Re, widely used in fluid dynamics. A combination of the output D with three inputs, e.g., ρ, U, d, leads to another Π group:

$$\Pi_1 = D/(\rho U^2 d^2),$$

which is commonly known as the drag coefficient C_d. From the above procedure, we make the following observations:

- Because there are 3 fundamental dimensions and 5 variables and parameters, there are 5 - 3 = 2 independent dimensionless Π groups for this problems.

- The Π groups are not unique; any product or quotient of any powers of the Π groups makes a new Π group, which is however not independent of the original 2. If we had tried to form a Π group from D, U, d and μ, for example, we would have ended up with $\Pi_3 = D/(\mu U d) = \Pi_1 \cdot \Pi_2$.

- The choice of which Π groups to use depends on the need of the problem and convention. A rule of thumb is to form one Π group for each of the output variables of interest. This facilitates the analysis and plotting of dimensionless data.

Now the pi theorem stipulates that the dependence of D on the inputs can be reduced to a simpler dependence among the Π groups: C_d = F(Re). In fact, graphs of the drag coefficient as a function of the Reynolds number are widely available on aircraft wings and other objects in air flows.

After we have measured D on the model airplane, how to use the dimensional analysis above to extrapolate it to the drag on the real airplane? If we ensure the same Re in the model experiment as in the flight of the real aircraft, then the pi theorem guarantees that C_d also be the same between the two. Thus, we have achieved similarity, and the drag force D_m measured on the model in the wind-tunnel experiment can be translated to the force D_p on the real airplane according to

$$\frac{D_m}{\rho_m U_m^2 d_m^2} = \frac{D_p}{\rho_p U_p^2 d_p^2},$$

where the subscript m refers to quantities in the model experiment, and p to those for the prototype. The beauty of similarity is that it works without our having to know the relationship between the "output", i.e., the drag force D in this case, and the input variables and parameters. In reality, such a dependence is usually complex and not known. In chemical and process engineering, this approach forms the foundation for scale-up of bench-top experiments to plant-scale reactors [2, 3]. It has also seen limited applications to bioreactors and living systems [1, 4].

To summarize the above procedure, we go through the following steps:

(a) Identify the key output function
(b) Identify the input variables and parameters
(c) Construct the dimensionless Π groups using dimensional analysis
(d) Establish similarity-scaling relations.

The same procedure readily applies to the scaling of an organ-on-a-chip (OoC), as an OoC is also a system with one or multiple outputs that depend on input variables and parameters. However, an OoC typically involves both mechanical and biochemical mechanisms, variables and parameters. Thus, it is likely more complex than the typical mechanical system, with a larger number of inputs and outputs. Moreover, greater complexities arise when multiple OoCs (MOoCs) are integrated into a body-on-a-chip system that models the crosstalk between multiple organs. However, this increase in complexity is incremental—a greater number of variables and parameters result in a greater number of Π groups, and greater practical challenges to ensure equality of all these Π groups between the model and the prototype. There is no qualitative difference in applying similarity scaling to MOoCs. In practice, complete similarity becomes rare for such

complex systems, and one may have to rely on partial similarity. The three case studies detailed below consist of two single OoCs and one MOoC.

Data for case study 1: lung-on-a-chip

Huh et al. [5] developed the lung-on-a-chip (LOAC) as a model for an alveolus. It consists of an air chamber and a microvascular chamber separated by a membrane-supported air-liquid interface (ALI). On the air side of the membrane, an epithelium is cultured with airway epithelial cells with proper mucus production. The vascular side of the membrane features an endothelial monolayer. A distinct feature of the device is that the membrane can be cyclically stretched at prescribed amplitude and frequency, thus replicating the alveolar stretching during breathing. Huh et al. [6] explored the use of LOAC as a disease model for pulmonary edema that arises during cancer treatment by interleukin-2 (IL-2). They observed that the concurrence of IL-2 at clinical dosage and stretching at proper frequency, amplitude and duration leads to gradual loss of the barrier function and increased permeability across the ALI (their Fig. 2B). The permeability is quantified by measuring the amount of fluorescein-conjugated inulin that crosses the ALI in time. The increased permeability is a hallmark of acute respiratory distress syndrome [7].

For dimensional analysis of the LOAC, we list the output and input variables:

- Membrane permeability k
- IL-2 volume fraction c
- Membrane stretching strain amplitude ε
- Stretching frequency f
- Duration of IL-2 application T
- Medium perfusion velocity V
- Total thickness of the ALI δ
- Chamber width D

The 8 quantities have 2 fundamental dimensions (length L and time T; note that permeability has dimension L^2 from Darcy's law), so we expect 6 dimensionless Π groups. They can be constructed methodically using the procedure outline in the above. But we can also take some shortcuts by recognizing that c and ε are dimensionless to begin with, and the other Π groups can be obtained from simple ratios or products:

$$\Pi_1 = k/D^2,\ \Pi_2 = c,\ \Pi_3 = \varepsilon,\ \Pi_4 = Tf,\ \Pi_5 = fD/V,\ \Pi_6 = \delta/D.$$

Let us examine the various similarity criteria and determine if they are satisfied in the LOAC. Alveolar diameter ranges from 200 to 500 microns [8], and the LOAC device has a membrane width of D = 400 microns. Thus, Huh et al. strove for a 1:1 scale in dimensions. The ALI thickness $\delta \sim 1$ μm also approximates the in vivo thickness. Thus, all the geometric features are matched to the alveolus, with

identical length ratios: Π_6 = *idem*, which is a shorthand for Π_6 being the same between the model and the prototype. The requirement of length ratios to be the same is known as geometric similarity [9]. When applied to cell cultures, the criterion of geometric similarity should be supplemented by morphological similarity, i.e., similar spatial arrangement of the different cell types. In the LOAC, the endothelial-epithelial membrane approximates the air-blood boundary in vivo, with a monolayer of endothelial or epithelial cells in confluence on either side. Therefore, morphological similarity is also satisfied.

Among the operating conditions, Huh et al. [6] have chosen the strain amplitude ε = 10% and frequency f = 0.2 Hz for the membrane stretching, and the medium perfusion rate V according to in vivo conditions. Thus, Π_3 = *idem* and Π_5 = *idem*. These quantities concern the flow and movement, and their similarity is known as kinematic similarity in engineering [9].

The IL-2 dosage c and application time T were also chosen to be the same as in vivo. We can call the similarity among quantities concerning the administration and metabolism of drugs metabolic similarity. Then Π_2 = *idem* and Π_4 = *idem*, and metabolic similarity is also observed.

Since all the input Π groups satisfy similarity: Π_i = *idem*, i = 2, . . . , 6, the membrane permeability must also obey similarity: Π_1 = *idem*, or k = idem since D = *idem*. Complete similarity is achieved; in fact, this happens to be a special case with 1:1 scaling. Huh et al. [6] reported good agreement between the in vitro permeability and ex vivo data on whole mouse lung. This serve as a successful example in support of the similarity scaling method.

Data for case study 2: liver-on-a-chip

The Liver-Chip is typical of many liver-on-a-chip devices that have appeared in recent years [10, 11]. As a mimic for a liver sinusoid, the chip's overall design resembles that of the LOAC in having a porous membrane separating two microfluidic chambers. The top (vascular) chamber has liver sinusoidal endothelial cells cultured atop the membrane, and is perfused by liquid medium. The bottom chamber features hepatocytes. In the study to be analyzed here, Ewart et al. [12] injected various drugs into the vascular chamber of the Liver-Chip device to study drug-induced liver injury (DILI). Of several indicators of DILI, the reduction in albumin production is a quantitative marker that can serve as the output in similarity analysis.

As in the above, we first identify the output and input variables:

- The ratio φ of albumin production under drug treatment to the baseline of no drugs
- Medium perfusion velocity u
- Initial drug molar concentration c

- Required drug concentration c_{50} to produce a 50% reduction in albumin, as an indication of the drug's potency
- Drug diffusivity in perfusate D
- Drug permeability through membrane P
- Drug clearance rate k
- Chamber dimension L

An obvious choice for the output function is the ratio of albumin production φ, which has no dimension to begin with: $\Pi_1 = \varphi$. The 7 input quantities contain 3 fundamental dimensions: length L, time T and amount of substance N (the molar concentration has dimension $\{c\} = \{c_{50}\} = NL^{-3}$). Thus we expect 4 Π groups which can be constructed following the standard procedure [1]. But shortcuts are available given the special features of the problem. An obvious Π group is the ratio of concentrations: $\Pi_2 = c/c_{50}$. To construct the remaining 3 Π groups, an intuitive way is to recognize the various time scales in the system:

$T_r = L/u$, residence time;

$T_c = cL^3/(ck) = L^3/k$, clearance time;

$T_d = L^2/D$, diffusion time;

$T_p = L/P$, permeation time.

Now we can obtain the 3 Π groups from the ratios of these time scales: $\Pi_3 = T_c/T_r = uL^2/k$, $\Pi_4 = T_d/T_r = uL/D$, $\Pi_5 = T_p/T_r = u/P$, where Π_3 and Π_4 can be identified respectively with the Damkhöler number and the Péclet number commonly used in chemical engineering processes [13]. In the following, we estimate the parameter values in vitro and in vivo to assess if similarity is achieved.

Geometry and morphology. The Liver-Chip has larger dimensions than the liver sinusoid in vivo, but this need not impair similarity scaling as long as the differing length scale is compensated for by the other parameters such that Π_3 and Π_4 are equal to those in vivo. On the chip, the functional surfaces are essentially planar 2D monolayers, whereas the liver sinusoid has a tubular structure. The difference in shape does not matter as long as the monolayer surface area and the total number of hepatocytes are properly scaled. From the dimension of the Liver-Chip, we have taken the length scale L = 200 μm in vitro [10, 12], compared with the in vivo dimension of 5 μm [14]. In terms of cell morphology, the Liver-Chip mimics the heterotypic cellular arrangement, using the proper ratio among the different cell types (e.g., hepatocytes, liver sinusoidal endothelial cells, stellate cells and Kupffer cells), and arranging them in a layered structure that functionally mimics the sinusoid [10, 12, 15]. Based on this, we can argue that morphological similarity is maintained.

Perfusion rate. To ascertain kinematic similarity, we evaluate the in vitro perfusion velocity u from the volume flow rate Q = 30 μL/hr [12] and the cross-sectional area A of the endothelial chamber of the Liver-Chip [10, 12]. This gives us the in

vitro velocity of 2500 μm/min. The in vivo velocity is inferred from the in vitro perfusion velocity of Prodanov et al. [11] and their statement that this velocity "is 2–3 orders of magnitude lower than in vivo values". We will take an intermediate ratio of 500. Their in vitro velocity is calculated from the perfusion rate Q = 1 μL/hr and the endothelial cross-sectional area A = 0.125 mm^2. Thus, the in vivo velocity u = 66.7 (mm/min).

Drug clearance rate. The liver clearance rate can differ by up to 2 orders of magnitude among different drugs [16]. For our purpose, we have chosen diclofenac as a representative because its clearance data are available [16, 17] and it is among the drugs tested by Ewart et al. [12]. The in vitro clearance rate for diclofenac is about 17 μL/min per 10^6 hepatocytes [17]. Then we ask how many hepatocytes are in the Liver-Chip of [12]. The endothelial chamber is 1 mm wide, 0.2 mm deep and 18 mm long [10]. The area of the hepatocyte-covered membrane is A = 18 mm^2. Given the cell diameter of 13.52 μm [18], the total number of hepatocytes in vitro is $N = 9.85 \times 10^4$. Now the in vitro clearance rate for the Liver-Chip is k = 1.67 μL/min. The in vivo k value for diclofenac is 418 mL/min per kg of human body weight [16]. Taking a 70-kg person with a total number of 1 billion sinusoids [14], we can estimate the in vivo clearance rate for a single sinusoid: $k = 2.93 \times 10^7$ μm^3 /min.

Transport coefficients. For the diffusivity in medium, a representative value for small-molecule drugs is $D = 4.5 \times 10^4$ μm^2/min [19]. For the permeability P, Leedale et al. have given a formula for calculating the "passive diffusion uptake" from the lipophilicity of the drug, in unit of μL/min per 10^6 hepatocytes. For a medium lipophilic drug, we can calculate the permeability through each hepatocyte of diameter of d = 13.52 μm [18], and then through the Liver-Chip with $N = 9.85 \times 10^4$ hepatocytes: $P = 6.53 \times 10^6$ μm/min. For D and P, we find no in vivo values, and thus have assumed the same values as in vitro.

Dosage. Ewart et al. [12] have tabulated the in vitro and in vivo doses in their Table S2. The c_{50} values for declofenac are taken from Chan et al. [20], which listed c_{50} = 0.05 μM or 0.15 μM in two different human whole blood assays. We have taken an intermediate value c_{50} = 1 μM.

These parameters are compiled in Table 1 of the main paper. The dimensionless groups show that similarity is achieved between the Liver-Chip and the liver sinusoid. This provides an explanation for the success of the chip in detecting DILI, as well as support to the similarity scaling approach.

Data for case study 3: gut-liver multi-organ-on-chip system

Cirit et al. [16, 17, 21] presented detailed pharmacokinetic data for a number of drugs in a gut-liver MOoC system, which captured the key functions of both organs and their crosstalk. We follow the same procedure as above, first identifying the output and input variables, then constructing the Π groups, and finally determining if the similarity criteria are satisfied.

This MOoC has multiple output variables, alongside a host of input variables:

- The output variables are the time-concentration profiles for drugs in different compartments of the system: $c_{ga}(t)$ in the apical chamber of the gut, $c_{gb}(t)$ in the basolateral chamber of the gut, $c_l(t)$ in the liver, and $c_m(t)$ in the mixing chamber
- Intrinsic drug clearance rates C_g for gut and C_l for liver
- Drug permeability through membrane P
- Fraction of unbound drug in circulating medium f_u
- Total perfusion rate Q, and its partition between the gut and liver
- Initial drug molar concentration c_0 in dosed chamber
- Geometric parameters: volumes V_{ga} (gut apical chamber), V_{gb} (gut basolateral chamber), V_l (liver chamber), V_m (mixing chamber); surface area of the gut membrane S

There are a total of 15 quantities in the list above, with 3 fundamental dimensions (length, time and amount of substance). Thus, we expect 12 dimensionless Π groups [1]. For the output variables, the 4 molar concentrations can be easily scaled to yield 4 Π groups by using the initial drug molar concentration:

$$\Pi_1 = c_{ga}/c_0, \Pi_2 = c_{gb}/c_0, \Pi_3 = c_l/c_0, \Pi_4 = c_m/c_0.$$

For the remaining 10 variables and constants, there are only two fundamental dimensions, length and time. Thus, we can define a characteristic length $L_0 = V_m^{1/3}$ and a characteristic time (the circulation time) $T = V_m/Q$, and readily obtain the remaining 8 dimensionless Π groups:

$$\Pi_5 = f_u, \Pi_6 = C_g/Q, \Pi_7 = C_l/Q, \Pi_8 = PS/Q,$$

$$\Pi_9 = V_{ga}/V_m, \Pi_{10} = V_{gb}/V_m, \Pi_{11} = V_l/V_m, \Pi_{12} = S/V_m^{2/3}.$$

The last one Π_{12} can be dropped since S only appears together with P in the drug mass transport, and thus PS can be viewed as a single parameter in the scaling exercise. In the following we estimate the parameter values in vitro and in vivo to assess if similarity is achieved.

Geometry and morphology. The in vitro geometric parameters are: V_{ga} = 0.5 mL, V_{gb} = 1.5 mL, V_l =1.4 mL, V_m = 1 mL, and S = 1.12 cm^2.

For the liver volume in vivo, we take V_l = 1500 mL [22]. There is some uncertainty as to how to interpret the other volumes in vivo. If we equate the gut with the small intestines, with an average length of 5 m [23] and diameter of 2.5 cm [24], we get a gut volume of V_{ga} = 2454 mL. Its surface area is S = 30 m^2 because of the surface ruffles due to the villi and microvilli [25]. The “basolateral chamber” of the gut in the OoC corresponds to the intestinal blood vessels, for which we did not find a volume. Thus, we will take V_{gb} to be the same as V_{ga} in vivo. Finally,

the “mixing chamber” should correspond to the systemic circulation for these 2 organs. The total amount of blood in the human body is roughly 5000 mL [26]. Since the liver and the gut account for, respectively, about 25% and 10% of the total cardiac output [27], we can take 35% of the total blood volume to be the in vivo counterpart of the mixing chamber volume: V_m = 1750 mL. Based on these values, we can compare the Π groups Π_9, …, Π_{12} (in vitro values followed by in vivo values in parentheses):

Π_9 = 0.5 (1.4), Π_{10} = 1.5 (1.4), Π_{11} = 1.4 (0.857), Π_{12} =1.12 (2066).

The volume ratios Π_9, Π_{10}, Π_{11} are reasonably close between in vitro and in vivo, but the surface area discrepancy (Π_{12}) is large. Since Π_{12} is unimportant to the scaling, as noted in the above, we can claim that the MOoC device has satisfied geometric similarity approximately.

In terms of cell composition and configuration, the MOoC strives to mimic the gut and liver in vivo. For example, the liver OoC used the in vivo ratio between the number of hepatocytes and Kupffer cells. Similarly, the gut OoC used realistic ratios among the epithelial, goblet and dendritic cells. The configuration of the liver OoC reflects the liver sinusoids in vivo, while the gut OoC mimics the epithelium in vivo. Thus, based on the available information, we can assume that morphological similarity is attained.

Drug clearance, transport and liquid perfusion rates. The key quantities are C_g, C_l, P and Q, and these are tabulated for the drug diclofenac in Table 2 of the main paper. The in vitro values are taken from [17]. Maas et al. [16] have cited in vivo values for C_l, but did not report any C_g value. In view of the much lower gut clearance in vitro, the in vivo value is expected to be low, and we have put it to zero. For the permeability P, Maas et al. reported an in vitro value but not an in vivo one. We have taken their in vitro value, which differs somewhat from that of [17], as in vivo. The in vivo perfusion rate is based on the hepatic blood flow [27] coming from both the artery and the portal vein. This is the proper counterpart of the in vitro flow rate in view of the flow rate partition scheme in the MOoC [16, 17].

Drug dosage. The last input Π group to be examined is $\Pi_5 = f_u$, the fraction of unbound drug in the circulating medium. Tsamandouras et al. [17, 21] cited f_u = 0.13 in both the gut and the liver in the MOoC device. We have not found in vivo values. If one uses the proper medium in vitro, f_u should be the same as in vivo. Thus, we assume that Π_5 = *idem* is satisfied.

Diclofenac time-concentration profiles. Of the 4 output Π groups, we have in vivo data only for the drug concentration in the plasma [16], which corresponds to the in vitro concentration in the mixing chamber [21]. Both correspond to $\Pi_4 = c_m/c_0$, which is compared in Figure 1 in the main text. To evaluate Π_4, we need the c_0 values in vitro and in vivo. In vitro, c_0 = 40 μM [21]. In vivo, Maas et al. [16] estimated $c_0 = FD_o/V_{ga}$, F being the drug’s bioavailability, D_o the dose

administered, and V_{ga} the volume of the dosing chamber (apical gut chamber). With F = 0.54, D_o = 50 mg [28], and V_{ga} = 2454 mL, we get the in vivo characteristic concentration in the gut: c_0 = 11 µg/mL.

In comparing the partial list of Π groups in Table 2, we have come to the conclusion that kinematic similarity is violated. This explains the failure of the liver-gut MOoC to recapitulate the in vivo drug concentration profile of Figure 1. Thus, this case study provides an example of how failing the kinematic similarity leads to failing the metabolic similarity. It illustrates the importance of similarity scaling from a negative result.

Note, however, that the failure being in a multi-organ system is a coincidence; the similarity scaling approach is not intrinsically limited to single-organ OoCs. In practical terms, MOoCs have a greater number of parameters and hence more Π groups. This does make complete similarity harder to achieve and increase the chance of a certain criterion being violated. Partial similarity may become a necessity for MOoCs.

References

1. Zlokarnik, M., *Scale-Up in Chemical Engineering*. 2nd edition ed. 2006: Wiley−VCH Verlag GmbH & Co. KGaA.
2. Bonem, J.M., *Chemical Projects Scale Up: How to Go from Laboratory to Commercial*. 2018: Elsevier.
3. Bisio, A. and R.L. Kabel, *Scale-up of Chemical Processes: Conversion from Laboratory Scale Tests to Successful Commercial Size Design*. 1985: Wiley-Interscience.
4. Nielsen, J., J. Villadsen, and G. Liden, *Scale-up of bioprocesses*, in *Bioreaction Engineering Principles*. 2003, Kluwer Academics. p. 477-518.
5. Huh, D., et al., *Reconstituting organ-level lung functions on a chip.* Science, 2010. **328**(5986): p. 1662-8.
6. Huh, D., et al., *A human disease model of drug toxicity-induced pulmonary edema in a lung-on-a-chip microdevice.* Sci Transl Med, 2012. **4**(159): p. 159ra147.
7. Batah, S.S. and A.T. Fabro, *Pulmonary pathology of ARDS in COVID-19: A pathological review for clinicians.* Respir Med, 2021. **176**: p. 106239.
8. Koeppen, B.A. and B.M. Stanton, *Introduction to the respiratory system*, in *Berne & Levy Physiology*. 2008, Mosby/Elsevier. p. 418-422.
9. White, F.M., *Dimensional analysis and similarity*, in *Fluid Mechanics*. 2011, McGraw-Hill. p. 293-345.
10. Peel, S., et al., *Introducing an automated high content confocal imaging approach for Organs-on-Chips.* Lab Chip, 2019. **19**(3): p. 410-421.

11. Prodanov, L., et al., *Long-term maintenance of a microfluidic 3D human liver sinusoid.* Biotechnol Bioeng, 2016. **113**(1): p. 241-6.
12. Ewart, L., et al., *Qualifying a human Liver-Chip for predictive toxicology: Performance assessment and economic implications.* bioRxiv, 2021: p. 2021.12.14.472674.
13. Bird, R.B., W.E. Stewart, and E.N. Lightfoot, *Transport Phenomena*. 2nd ed. 2006: Wiley-VCH.
14. Mak, K.M. and D.W. Shin, *Hepatic sinusoids versus central veins: Structures, markers, angiocrines, and roles in liver regeneration and homeostasis.* Anat Rec (Hoboken), 2021. **304**(8): p. 1661-1691.
15. Sphabmixay, P., et al., *High resolution stereolithography fabrication of perfusable scaffolds to enable long-term meso-scale hepatic culture for disease modeling.* Biofabrication, 2021. **13**(4).
16. Maass, C., et al., *Multi-functional scaling methodology for translational pharmacokinetic and pharmacodynamic applications using integrated microphysiological systems (MPS).* Integr Biol (Camb), 2017. **9**(4): p. 290-302.
17. Tsamandouras, N., et al., *Integrated Gut and Liver Microphysiological Systems for Quantitative In Vitro Pharmacokinetic Studies.* Aaps j, 2017. **19**(5): p. 1499-1512.
18. Li, R., et al., *Permeability comparison between hepatocyte and low efflux MDCKII cell monolayer.* Aaps j, 2014. **16**(4): p. 802-9.
19. Leedale, J.A., et al., *Multiscale modelling of drug transport and metabolism in liver spheroids.* Interface Focus, 2020. **10**(2): p. 20190041.
20. Chan, C.C., et al., *Rofecoxib [Vioxx, MK-0966; 4-(4'-methylsulfonylphenyl)-3-phenyl-2-(5H)-furanone]: a potent and orally active cyclooxygenase-2 inhibitor. Pharmacological and biochemical profiles.* J Pharmacol Exp Ther, 1999. **290**(2): p. 551-60.
21. Tsamandouras, N., et al., *Quantitative Assessment of Population Variability in Hepatic Drug Metabolism Using a Perfused Three-Dimensional Human Liver Microphysiological System.* J Pharmacol Exp Ther, 2017. **360**(1): p. 95-105.
22. Andersen, V., et al., *The volume of the liver in patients correlates to body weight and alcohol consumption.* Alcohol Alcohol, 2000. **35**(5): p. 531-2.
23. Teitelbaum, E.N., et al., *Intraoperative small bowel length measurements and analysis of demographic predictors of increased length.* Clin Anat, 2013. **26**(7): p. 827-32.
24. Jacobs, S.L., et al., *Small bowel faeces sign in patients without small bowel obstruction.* Clin Radiol, 2007. **62**(4): p. 353-7.
25. Helander, H.F. and L. Fändriks, *Surface area of the digestive tract - revisited.* Scand J Gastroenterol, 2014. **49**(6): p. 681-9.
26. Sharma, R. and S. Sharma, *Physiology, Blood Volume*. 2022, StatPearls Publishing.
27. Granger, D.N. and P.R. Kvietys, *Circulation, overview*. Encyclopedia of Gastroenterology, ed. L.R. Johnson. 2004, New York: Elsevier. 351-355.

28. Willis, J.V., et al., *The pharmacokinetics of diclofenac sodium following intravenous and oral administration.* Eur J Clin Pharmacol, 1979. **16**(6): p. 405-10.